



**REGION II**  
**UNIVERSITY TRANSPORTATION RESEARCH CENTER**

---

---

# **Final Report**

---

---

## **Three-dimensional Analysis of Underground Tunnels in Liquefiable Soil subject to Earthquake Loading**

Prepared by

**Huabei Liu**

Assistant Professor, Department of Civil Engineering  
The City College of New York/CUNY  
160 Convent Ave. ST 195  
New York, NY 10031,  
Tel: 212-650-8397  
Email: [hbliu@ce.ccny.cuny.edu](mailto:hbliu@ce.ccny.cuny.edu)

**January 11, 2011**



## **Disclaimer**

The contents of this report reflect the views of the authors, who are responsible for the facts and the accuracy of the information presented herein. The contents do not necessarily reflect the official views or policies of the UTRC or the Federal Highway Administration. This report does not constitute a standard, specification or regulation. This document is disseminated under the sponsorship of the Department of Transportation, University Transportation Centers Program, in the interest of information exchange. The U.S. Government assumes no liability for the contents or use thereof.

1. Report No.		2. Government Accession No.		3. Recipient's Catalog No.	
4. Title and Subtitle Three-dimensional Analysis of Underground Tunnels in Liquefiable Soil subject to Earthquake Loading				5. Report Date January 11, 2011	
				6. Performing Organization Code	
7. Author(s) Huabei Liu, the City College of New York				8. Performing Organization Report No. 49111-15-20	
9. Performing Organization Name and Address The City College of New York 160 Covent Avenue New York, NY 10031				10. Work Unit No.	
				11. Contract or Grant No.	
12. Sponsoring Agency Name and Address University Transportation Research Center Marshak Hall, Room 910 The City College of New York New York, NY 10031				13. Type of Report and Period Covered Final Report	
				14. Sponsoring Agency Code	
15. Supplementary Notes					
16. Abstract  Underground tunnels pass through complicated ground that may consist of both liquefiable and nonliquefiable soils under seismic loading. This difference in liquefaction susceptibility would then lead to different development of excess pore pressure and different decreases of soil stiffness and strength, resulting in complicated three-dimensional deformation and damage of tunnels, the knowledge of which is still not well understood at present. In this study, three dimensional (3D) Finite Element analyses were carried out to investigate the seismic response of underground tunnels subject to earthquake loading, focusing on the 3D response of underground tunnels passing through both saturated dense and loose grounds. Twin subway tunnels at a diameter of 5 meter, the lining of which was made of grey cast-iron at a thickness of 6.5 cm, were considered in this study. It was found that underground tunnels passing through both dense and loose saturated ground exhibited two distinctive deformation modes: the uplift and the lateral deformation due to the difference in the soil liquefaction susceptibility. The tunnels were twisted due to these distinctive deformation modes and the maximum stress in the tunnels occurred at the boundary between dense and loose grounds. It was also found that when soil liquefaction was not extensive in the ground, the tunnels settled instead of uplifted. Different frequency characteristics of input motions resulted in significantly different responses of the ground-tunnel system, which was also related to soil thickness above bedrock. Synthesized motions from the same design response spectrum might still result in different stresses in the tunnels, indicating that in the design of underground tunnels sufficient number of synthesized motions compatible with the design spectrum should be analyzed in order to take into account the ground motion uncertainty.					
17. Key Words Underground tunnels, soil liquefaction, Finite Element method, 3D dynamic response, deformation Mode			18. Distribution Statement		
19. Security Classif. (of this report) Unclassified		20. Security Classif. (of this page) Unclassified		21. No of Pages 25	22. Price

# Three-dimensional Analysis of Underground Tunnels in Liquefiable Soil subject to Earthquake Loading

Huabei Liu

Assistant Professor, Department of Civil Engineering, City College of New York/CUNY  
160 Convent Ave. ST 195, New York, NY 10031, USA

Email: [hbliu@ce.ccny.cuny.edu](mailto:hbliu@ce.ccny.cuny.edu)

## **Abstract:**

Underground tunnels pass through complicated ground that may consist of both liquefiable and non-liquefiable soils under seismic loading. This difference in liquefaction susceptibility would then lead to different development of excess pore pressure and different decreases of soil stiffness and strength, resulting in complicated three-dimensional deformation and damage of tunnels, the knowledge of which is still not well understood at present. In this study, three dimensional (3D) Finite Element analyses were carried out to investigate the seismic response of underground tunnels subject to earthquake loading, focusing on the 3D response of underground tunnels passing through both saturated dense and loose grounds. Twin subway tunnels at a diameter of 5 meter, the lining of which was made of grey cast-iron at a thickness of 6.5 cm, were considered in this study. It was found that underground tunnels passing through both dense and loose saturated ground exhibited two distinctive deformation modes: the uplift and the lateral deformation due to the difference in the soil liquefaction susceptibility. The tunnels were twisted due to these distinctive deformation modes and the maximum stress in the tunnels occurred at the boundary between dense and loose grounds. It was also found that when soil liquefaction was not extensive in the ground, the tunnels settled instead of uplifted. Different frequency characteristics of input motions resulted in significantly different responses of the ground-tunnel system, which was also related to soil thickness above bedrock. Synthesized motions from the same design response spectrum might still result in different stresses in the tunnels, indicating that in the design of underground tunnels sufficient number of synthesized motions compatible with the design spectrum should be analyzed in order to take into account the ground motion uncertainty.

## **Keywords:**

Underground tunnels, soil liquefaction, Finite Element method, 3D dynamic response, deformation mode

## 1 Introduction

Underground structures in saturated soils may be subjected to severe damages during earthquake. One of the causes is the relative deformation of underground structures due to soil liquefaction. Underground tunnels or pipelines, for example, may be subjected to very large shear load if part of the tunnels or pipelines are in liquefiable soils and prone to upward and lateral movements while the other in non-liquefiable ones. The shear load may exceed the shear strength of the underground structures, resulting in severe damages.

The soil liquefaction induced uplift movement of underground pipelines during strong earthquake was firstly observed in 1964 Niigata Earthquake in Japan [1]. Similar damages were also found in recent earthquakes, including the 1989 Loma Prieta Earthquake [2], 1993 Hokkaido–Nansei–Oki Earthquake [3], 1994 Hokkaido–Toho–Oki Earthquake [4], 1995 Kobe Earthquake [5] and 1999 Taiwan Earthquake [6]. Reports on the damage to large underground structures due to liquefaction-induced uplift movement were scarce but still exist [7].

There have been extensive studies concerning the uplift behavior of pipelines due to earthquake-induced soil liquefaction. These studies include analytical and numerical analyses (e.g. [8]) as well as experimental investigations (e.g. [9], [10] and [11]). Comparatively fewer investigations can be found concerning the uplift or settlement of large underground structures such as subway and highway tunnels due to soil liquefactions. The investigations by Khoshnoudian Shahrour [12], Yang et al. [13], Taylor et al. [14], Liu and Song [15,16], Azadi and Mir Mohammad Hosseini [17,18], and Chou et al. [19] are the ones that worth mentioning. From these studies, the uplift of underground structures was found to consist of four mechanisms: ratcheting of underground structure, pore water migration, bottom heave due to shearing of soft non-liquefiable soil below underground structures, and flow deformation of liquefied soil, as summarized in Chou et al. [19]. Chou et al. [19] also found that under small seismic loading and when the excess pore pressure is not adequately large to cause extensive soil liquefaction, underground structures settle instead of uplift. Uplift occurred when the seismic loading was large. Studies also found that underground structures settle due to the soil consolidation following soil liquefaction [16,20]. Countermeasures to uplift or settlement were also studied, among which, gravel drainage [10,14], grouting [15,20] and cut-off walls [16,21-23] were found to be effective.

Concerning the transverse damage due to lateral soil deformation under seismic loading, studies so far have mainly focused on underground structures in non-liquefiable soils [e.g. 24-28]. Most of these studies were initiated following the extensive damage of the subway system in the 1995 Kobe earthquake [29]. Based on these studies, methods to analyze and design against the transverse damage of tunnel sections have been proposed [e.g.22]. In contrast, although liquefiable soil may result in much larger lateral deformation, the associated damage has seldom been investigated [16, 19].

Furthermore, in order to understand the full picture of the liquefaction response of underground tunnels under seismic loading, three-dimensional (3D) model testing or numerical simulation is

necessary but such studies are very rare at present. Specifically, investigating the damage of underground tunnels at the boundary of liquefiable and non-liquefiable soils as indicated in the first paragraph of this paper requires sophisticated and large-scale 3D modeling.

In this paper, three-dimensional numerical simulations were carried out to investigate the responses of subway tunnels in a ground that consisted of soils with different liquefaction susceptibilities. Particularly, different ground conditions were considered along the axial directions of the tunnels. The studies targeted twin subway tunnels in saturated soils. Low grade cast iron was used extensively as tunnel linings in the last two centuries, an example of which was the subway and highway tunnels in New York City [e.g. 30]. The tunnel lining was therefore assumed to be made of low-grade cast iron in this study. The study focused on the 3D deformation mechanism of underground tunnels, and the effects input ground motions and soil thickness were also investigated.

## 2 FINITE ELEMENT MODELS

In this study, the Finite Element program, TNO-DIANA9.4.2 [31] was used to investigate the problem. The program has the capacity to consider 3D soil liquefaction and earthquake input. The ground was simulated using the Nishi soil liquefaction model [32] that is incorporated in the Finite Element program and is capable of describing excess pore pressure built-up and soil liquefaction; the soil-tunnel interaction was modeled using interface elements, which is also one of the intrinsic functions of TNO-DIANA 9.4.2. The cast-iron tunnels were assumed to follow elastic perfectly-plastic behavior. Appendices I and II provide brief descriptions of the Nishi soil liquefaction model and the interface elements.

In order to model the different liquefaction susceptibilities, a loose soil and a dense soil were used in the analyses. The loose soil is a medium sand with a shear wave velocity of 110 m/s at a depth of around 4 meter, the saturated unit weight of which is 19 kN/m<sup>3</sup>; the dense soil is the Leighton Buzzard sand (120/200) at a relative density of  $D_r = 60\%$ , the saturated unit weight of which is 19.9 kN/m<sup>3</sup>. The two set of parameters were both identified by a TNO team on behalf of the Japanese Liquefaction User Group [33]. Table 1 summarizes the model parameters for the soils. The soils were assumed to follow undrained response during seismic loading, which is approximate but considering the short duration of seismic loading, it was still able to capture the main response of the saturated sand - tunnel system.

Table 1 Nishi model parameters for soils

	$\kappa^*$	$\nu$	$\phi$ (°)	$\phi_F$ (°)	$m^*$ (m <sup>2</sup> /N)	$n$	$G_0$	$\beta_1$
Loose sand	0.0025	0.3	30	28	$3.0 \times 10^{-5}$	3	1200	1500
Dense sand	0.003	0.3	39	32	$6.0 \times 10^{-4}$	3	2400	50

The soil-tunnel interface was assumed to have small friction of  $\sin\delta = 0.3$  in order to mobilize possible significant tunnel movement in the vertical direction. A small cohesion of 5 kPa was considered in the model to improve numerical stability. The thickness of interface elements in this study was unified as 1.0 cm, and their normal stiffness assumed a large value in order to prevent interface penetration while the shear stiffness was derived from the shear modulus of adjacent soil [31]. The Young's modulus, Poisson's ratio and yield strength of tunnel lining assumed typical values of low-grade grey cast-iron, which are  $E = 67 \text{ GPa}$ ,  $\nu = 0.28$  and  $\sigma_y = 150 \text{ MPa}$ . Material damping can mainly be captured by the soil models, hence only a small viscous damping of  $\xi=3\%$  was introduced in the analysis.

Twin subway tunnels, the inner diameter of which was 5.0 m and the equivalent thickness of which was 6.5 cm was analyzed in this study. The tunnels were assumed to be constructed at a depth of 5.5 m and their distance was assumed to be 9.0 m from center to center. The tunnel parameters were obtained from a real subway line in New York City [34]. The tunnels ran through a saturated ground that consisted of both loose and dense soils, the thicknesses of which in the vertical directions were both 15 meters. These two layers of soils were underlain by either bedrock or a dense soil layer at a thickness of 9 meter over bedrock. The ground motion was input at the bedrock. Fig. 1 illustrates the general setup of the Finite Element models with thick soil layers.

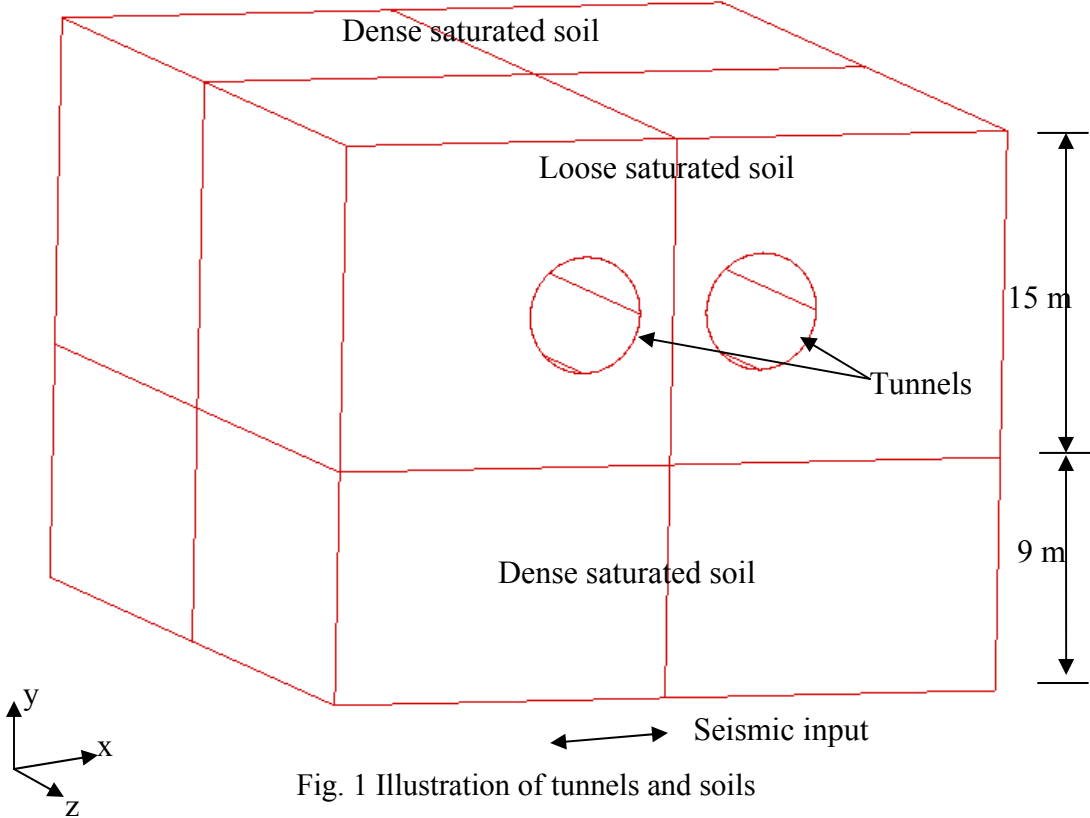


Fig. 1 Illustration of tunnels and soils

Two sets of ground motions were used as input. One was a record from the 1994 Northridge earthquake in California; the other set was the design seismic motion for New York City bridges proposed by Risk Engineering [35]. The two sets of motions were both scaled to a max acceleration of 0.35 g. In order to save analysis time, the motions were truncated to include only the main events. Fig. 2 shows the two sets of motions. It should be noted that two New York City motions were used. They were both compatible acceleration time-histories obtained from the design response spectrum for an earthquake return period of 2500 years. It can be seen that the dominant period of the California motion is much larger than that of the New York motions. The motions were input at the base the Finite Element models in the horizontal direction, perpendicular to tunnel axes, as shown in Fig. 1.

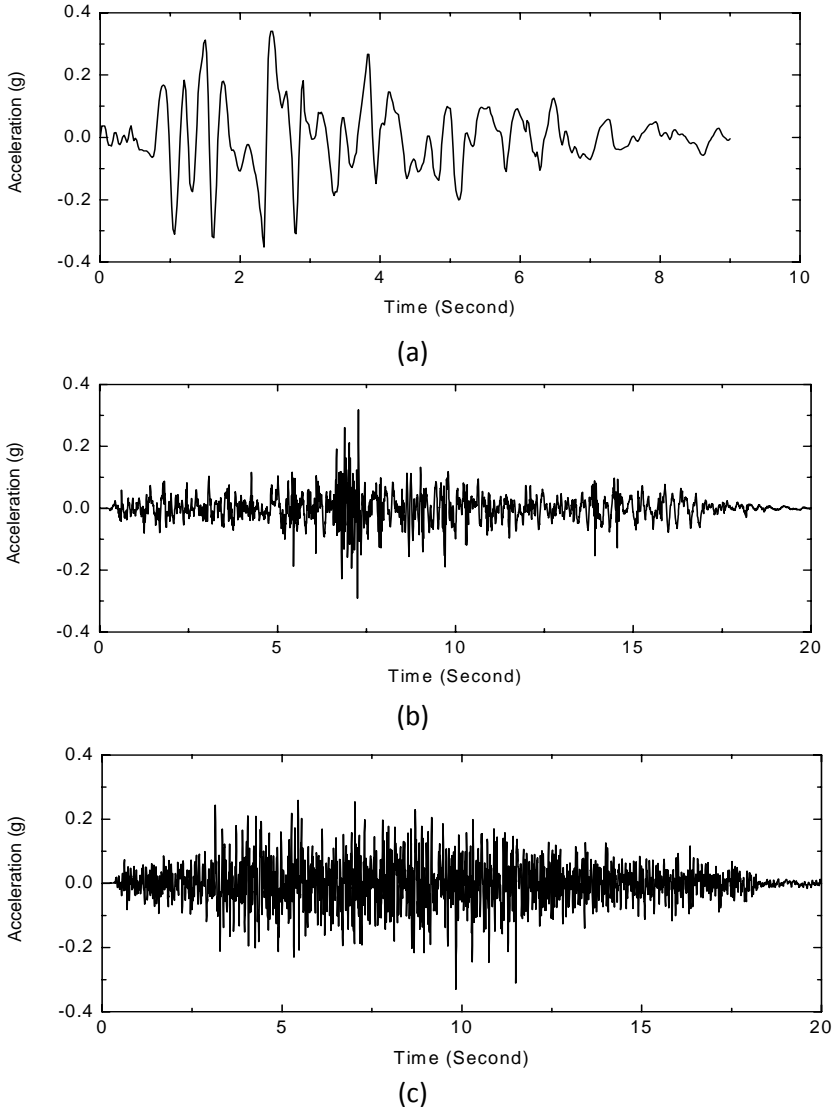


Fig. 2 Input ground motions: (a) one record from 1994 Northridge earthquake; (b) New York City synthesized motion I; (c) New York City synthesized motion II

### 3 Determination of the Finite Element Mesh Parameters

Twenty-node brick elements and curved shell elements were used to model the soils and tunnel linings, respectively. In order to determine the element size in the vertical directions, which would affect the shear wave propagation in this study, 3D models consisting only one element in the z direction as defined in Fig. 1 were analyzed. The models did not include the tunnels but include the loose soil on the top and the dense soil at the bottom as shown in Fig. 1, simulating the free-field response of the ground. Three element thicknesses, 1.0 m, 1.5 m and 2.0 m, were analyzed. Fig. 3 shows the comparison of accelerations at the ground surface with the input motions as shown in Fig. 2a and Fig. 2b. The accelerations were very close. A thickness of 2.0 m for one twenty-node brick element was therefore considered to be adequate in this study and it was used throughout the following analyses.

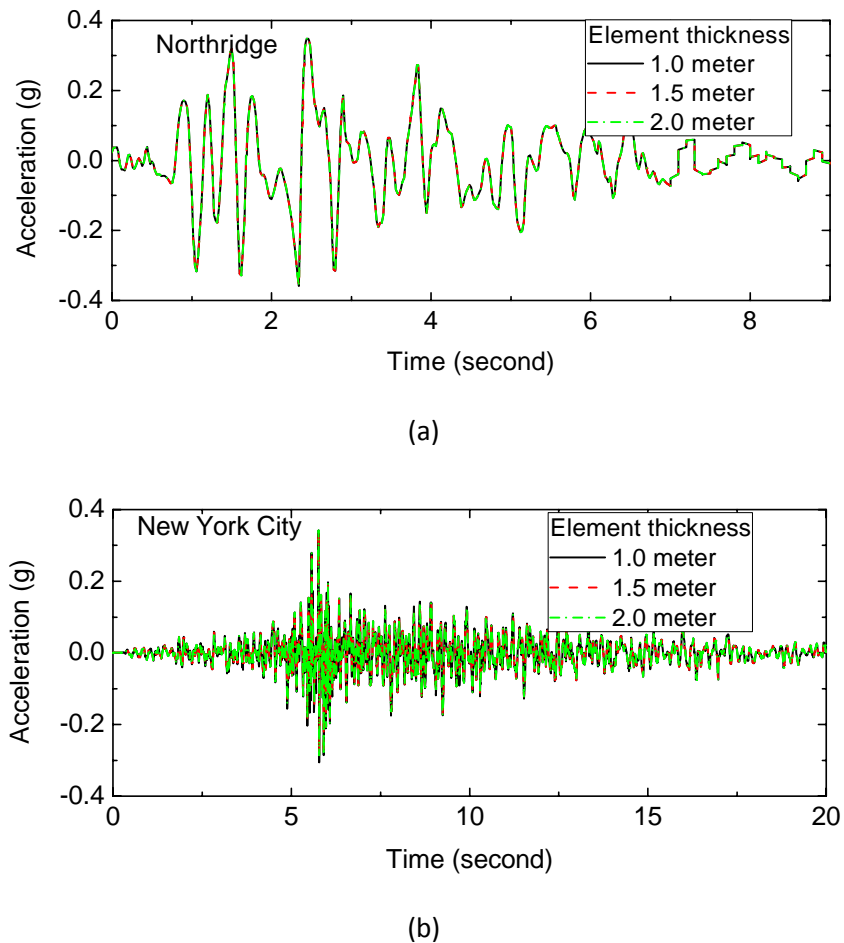
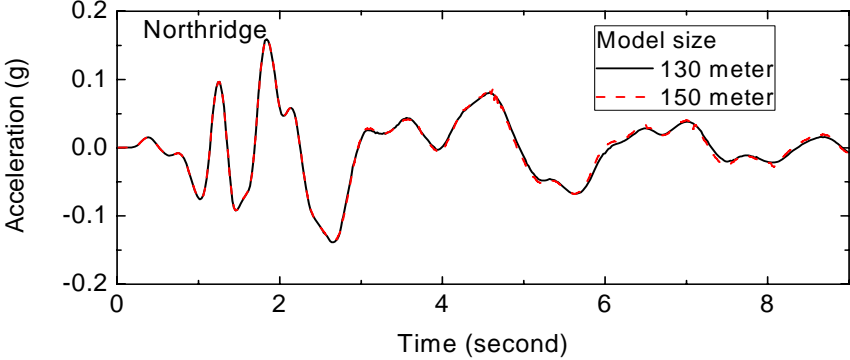


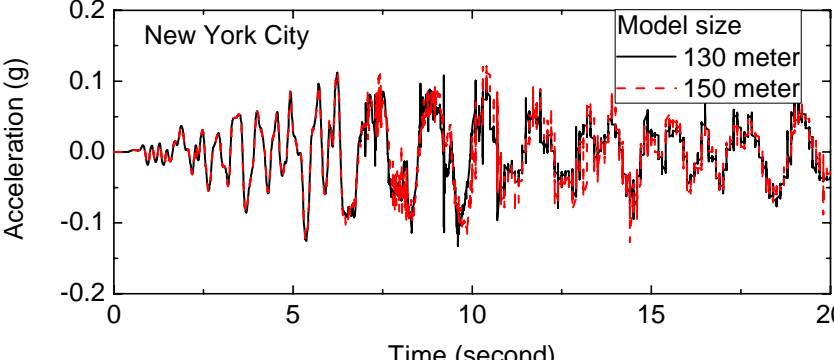
Fig. 3 Effects of element size in the vertical directions on the acceleration response on ground surface: (a) Northridge motion; (b) New York City motion 1

After determining the element size in the vertical direction, trial analyses were carried out to obtain the optimal dimensions of Finite Element mesh in the x direction as defined in Fig. 1. In

this study, the nodes on the left and right sides of the model, which were parallel to the tunnel axes, were tied to have the same displacements in order to simulate free field response under seismic loading [31]. However, the shear wave might still reflect from these boundaries and affect the response of the soil-tunnel system. Sufficiently large Finite Element domain is required in the x direction to diminish the influence. For this purpose, 3D Finite Element models, including the tunnels, with two layers of soil in the y direction but having only one element in the z direction, were analyzed. The models were fixed in the z direction on the front and back boundaries, simulating "plane strain" response, but the dimension in the x direction were varied to investigate the influence. It was found that with a dimension of 130 meter in the x direction, the model was sufficiently large to capture the free field response and the effect of tied boundary on the seismic response of the ground-tunnel system was already very small. Fig. 4 shows the comparison of horizontal accelerations at a point close to the tunnels, for a model of 150 meter and one of 130 meter. The difference can be considered to be sufficiently small.



(a)



(b)

Fig. 4 Effects of Finite Element mesh dimension in the transverse direction of tunnels: (a) Northridge motion; (b) New York City motion I.

The last parameter of the Finite Element mesh is the length along the longitudinal direction of tunnels. It should also be sufficiently long to fully capture the 3D tunnel responses under seismic loading. Particularly, the front and back boundaries should be sufficiently far away from the boundary of loose and dense grounds as shown in Fig.1. For this purpose, several models were analyzed and the stresses in the tunnels were compared. It was found that when the length of the model was 68 m, i.e. the distance from the front or back boundary to the boundary between two soils was respectively 34 m, the 3D responses of the tunnel could be fully captured. Fig. 5 shows the tunnel deformation subject to the Northridge motion at 6 second. Except for few localized regions, the two layer of lining elements close to the front or back boundaries had similar stresses, indicating that the 3D effects in the region around the soil boundaries had minimized and the tunnels began to behave as though the other layer of soil did not exist. This dimension was considered to be adequate and was used in the following analyses. Fig. 6 shows the Finite Element mesh of a deep model. The Finite Element model was fixed at the base, tied on the left and right boundaries and was prevented to displace in the z direction on the front and back boundary. The shallow models were the same as the deep ones in the x and z directions except that they were only 15 m thick in the y direction. The deep model had altogether 3780 elements and 16569 nodes while the shallow model had 2660 elements and 11625 nodes.

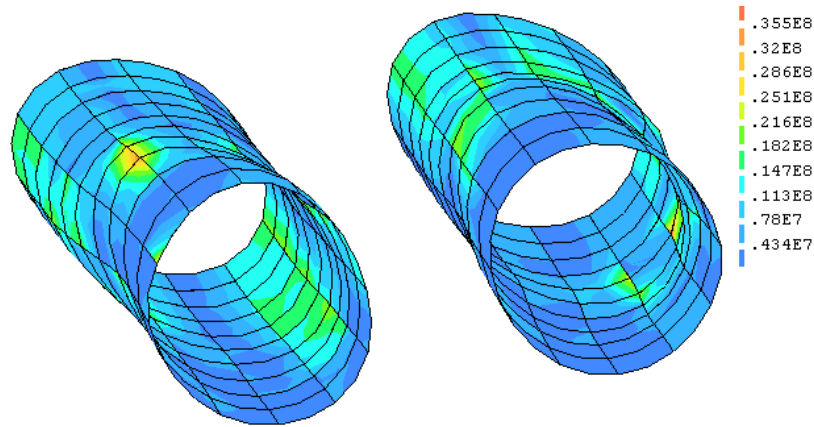


Fig. 5 von Mises stress in the tunnels at 6 second under the Northridge excitation

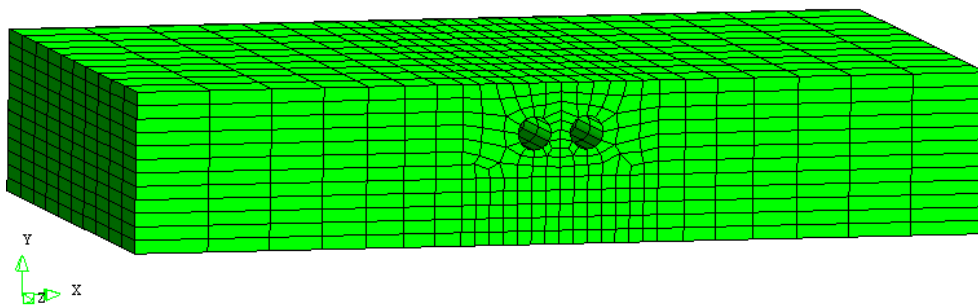


Fig.6 Finite Element mesh for the deep models

#### 4 Three-dimensional Deformations of Twin Tunnels under Seismic Loading

Comparatively the response of tunnels under the excitation of the Northridge motion was larger. The results of a shallow model subjected to the Northridge motion were used herein to discuss the 3D deformation mechanisms. Fig. 7 shows the deformed mesh at different instants and facing different directions. It can be seen clearly that under the 0.35g Northridge motion, the loose ground significantly liquefied, which led to two distinct deformation modes, heave of ground surface above the tunnels and lateral spreading of liquefied soils, as shown in Fig. 7a and 7b. On the other hand, the deformation of the dense ground was much smaller, as shown in Fig. 7c and 7d. This difference was of course due to the difference in pore water pressure build-up in the soils, as compared in Fig. 8. For the dense ground, only in the very top layer that the excess pore pressure ratio ( $\Delta u/\sigma_{v0}'$ ) was close to unity, while in almost the whole loose ground  $\Delta u/\sigma_{v0}'$  was close to unity, indicating total soil liquefaction. Fig. 9 shows the vertical displacement of tunnel sections with time. The vertical uplift on the loose soil side was quite large, while the tunnel section in the dense ground overall settled slightly. Fig. 9 also indicates that the tunnels ratcheted under the seismic loading and soil liquefaction, which was also observed in the centrifuge tests in Chou et al. [19] and was the main reason for underground structure uplift under modest earthquake-induced soil liquefaction.

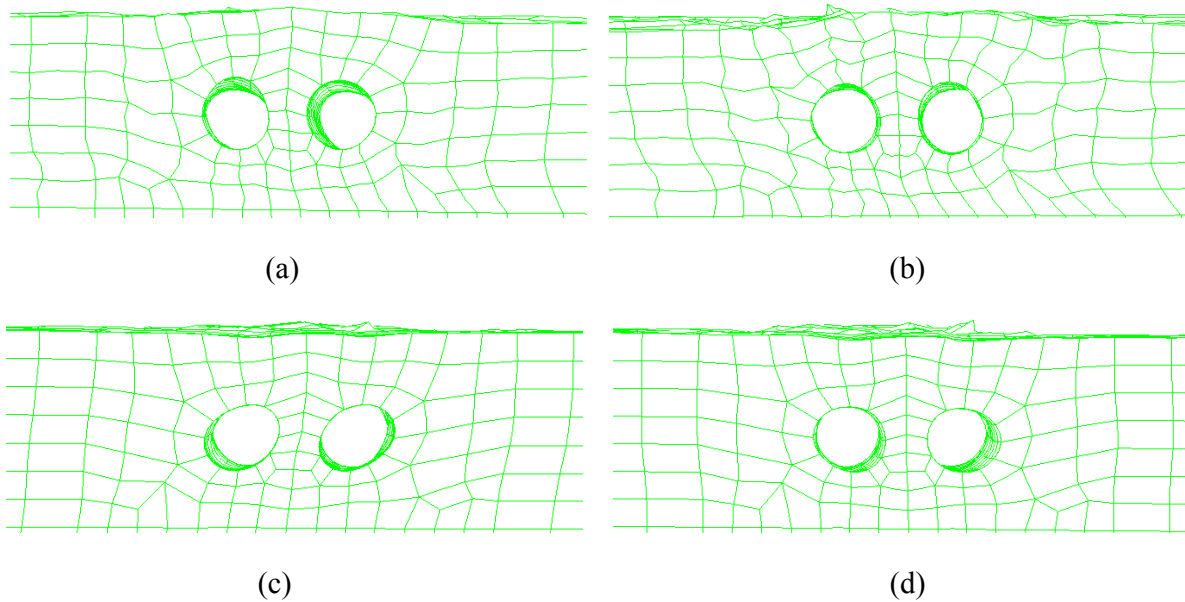


Fig. 7 Deformed Finite Element mesh (enlarged 35 times): (a) Front at 6 second; (b) Front at 9 second; (c) Back at 6 second; (d) Back at 9 second

The deformation characteristics of the ground were directly related to the deformation and stress in the subway tunnels, as shown in Fig. 10. Overall the tunnels were twisted due to the different vertical and lateral deformations in the dense and loose grounds. Comparatively the effect of lateral soil deformation was more considerable. The circular linings became oval-shaped due to lateral soil deformation. The maximum von Mises stress in the tunnels always occurred at a locations close to

the boundary of the loose and dense grounds and the largest value was found to occur at 4.56 second under the Northridge motion, which was around 50 MPa, as shown in Fig. 10a. It was still smaller than the assumed strength of tunnel lining in this study.

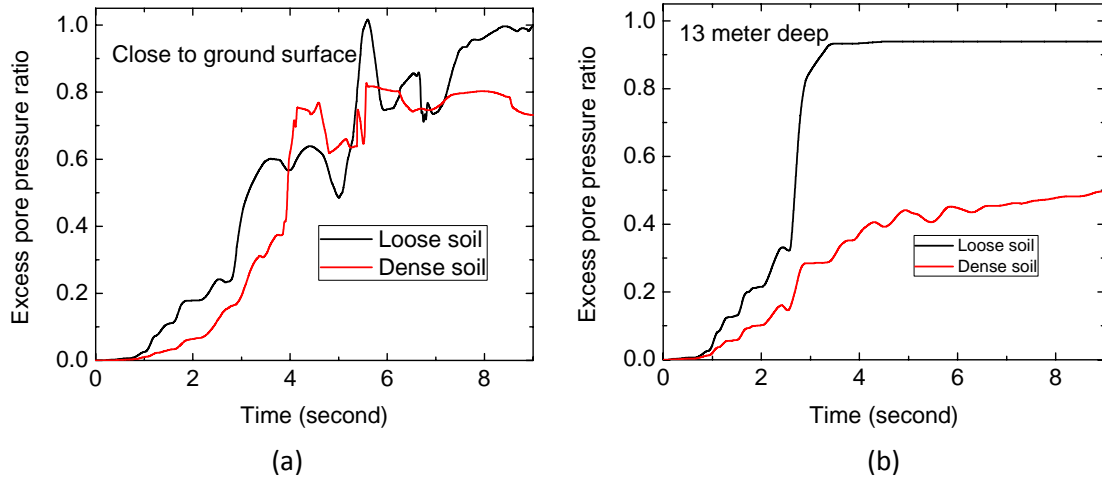
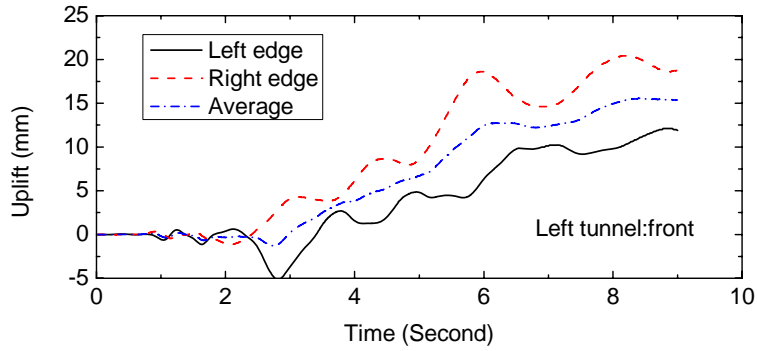
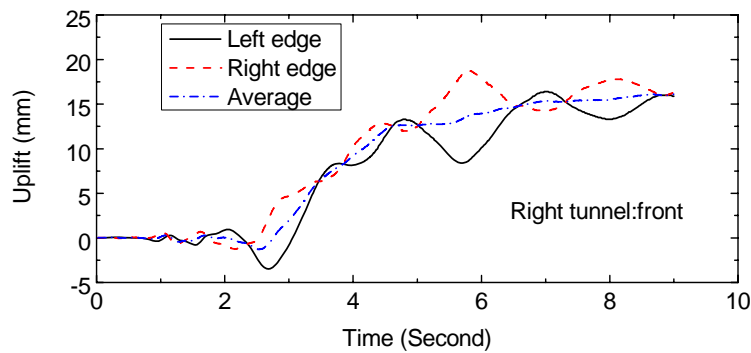


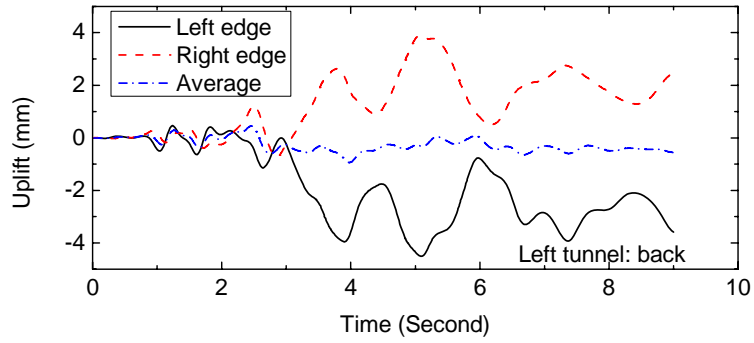
Fig. 8 Comparisons of excess pore pressure ratios ( $\Delta u/\sigma_0$ )



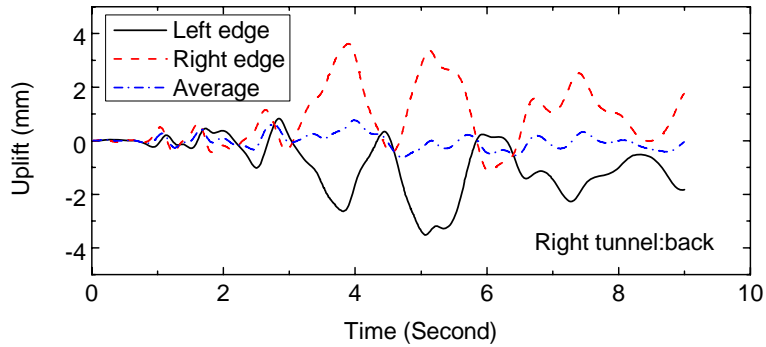
(a)



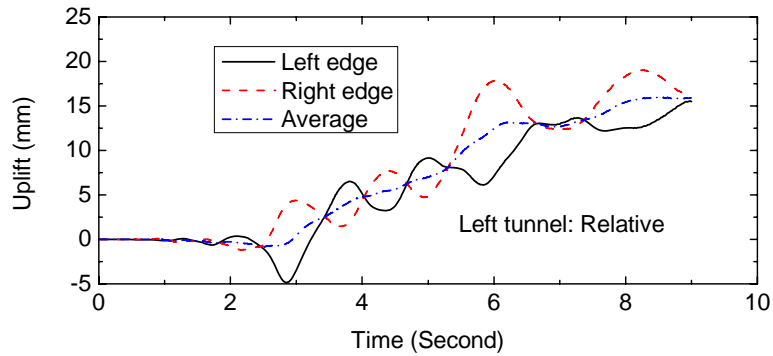
(b)



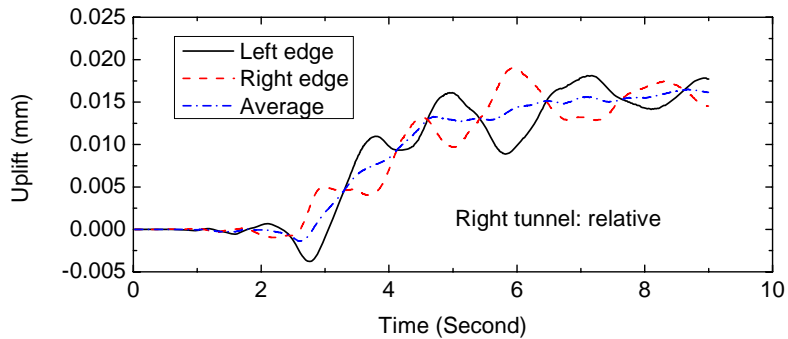
(c)



(d)



(e)



(f)

Fig. 9 Uplift of tunnel sections

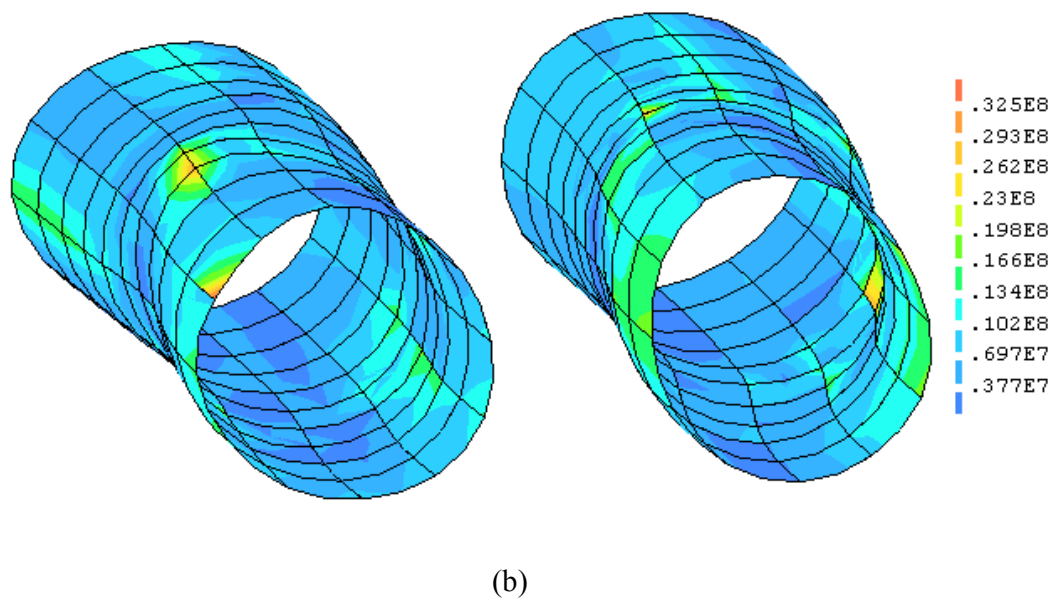
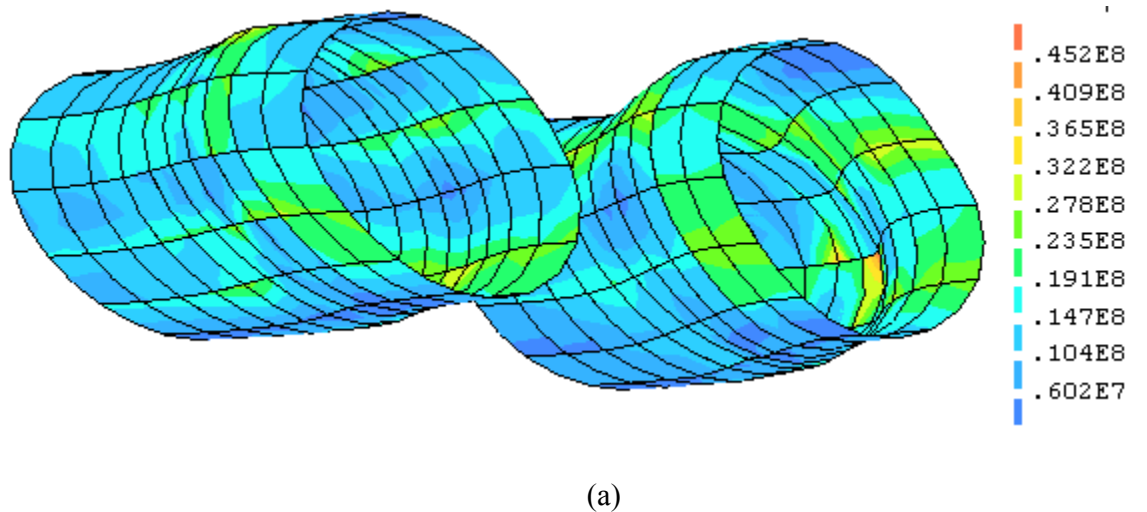


Fig. 10 Tunnel deformation and Mises stress: (a) At 4.56 second; (b) At 9 second  
(Deformation enlarged 35 times)

## 5 Effects of Input Ground Motions

Although having the same maximum accelerations, the Northridge motion resulted in much larger response in the ground and tunnels than the New York motions. This is understandable since ground response and soil liquefaction is closely related to the input motion frequency as well as the ground characteristics such as soil thickness and soil stiffness. In this case, development of excess pore pressure decreased the soil stiffness, hence increase the natural period of soil layers. The Northridge motion has much larger dominant period, and it would trigger larger response in the ground-tunnel system, including soil liquefaction, tunnel deformation and tunnel stress. Fig. 11 shows some of the

responses of the system under the excitation of New York motion I. The maximum stress still occurs close to the boundary of dense and loose grounds but the overall relative deformation in the vertical direction was very small and was negative. Under New York motion II, the excess pore pressure and vertical deformation of tunnels were very similar to those with New York motion I. However, there was still difference in the lateral deformation of soils, which led to smaller von Mises stress in the tunnels, as shown in Fig. 12.

The two New York motions were synthesized from the design response spectrum, hence they had very similar frequency characteristics, maximum accelerations and durations. However, the tunnel stress was still somewhat different, although much smaller than the difference between the New York motions and Northridge motion. The maximum Mises stress due to New York Motion I was more than 12 MPa while that due to New York motion II was less than 11 MPa. This difference indicates that, in the seismic design of underground structures, selection of input motions is critical; and sufficient number of motions that share similar response spectrum and durations should be used to adequately consider the motion uncertainty and to capture the envelope responses, similar to the design of buildings and bridges as specified by NEHRP [36] and AASHTO [37].

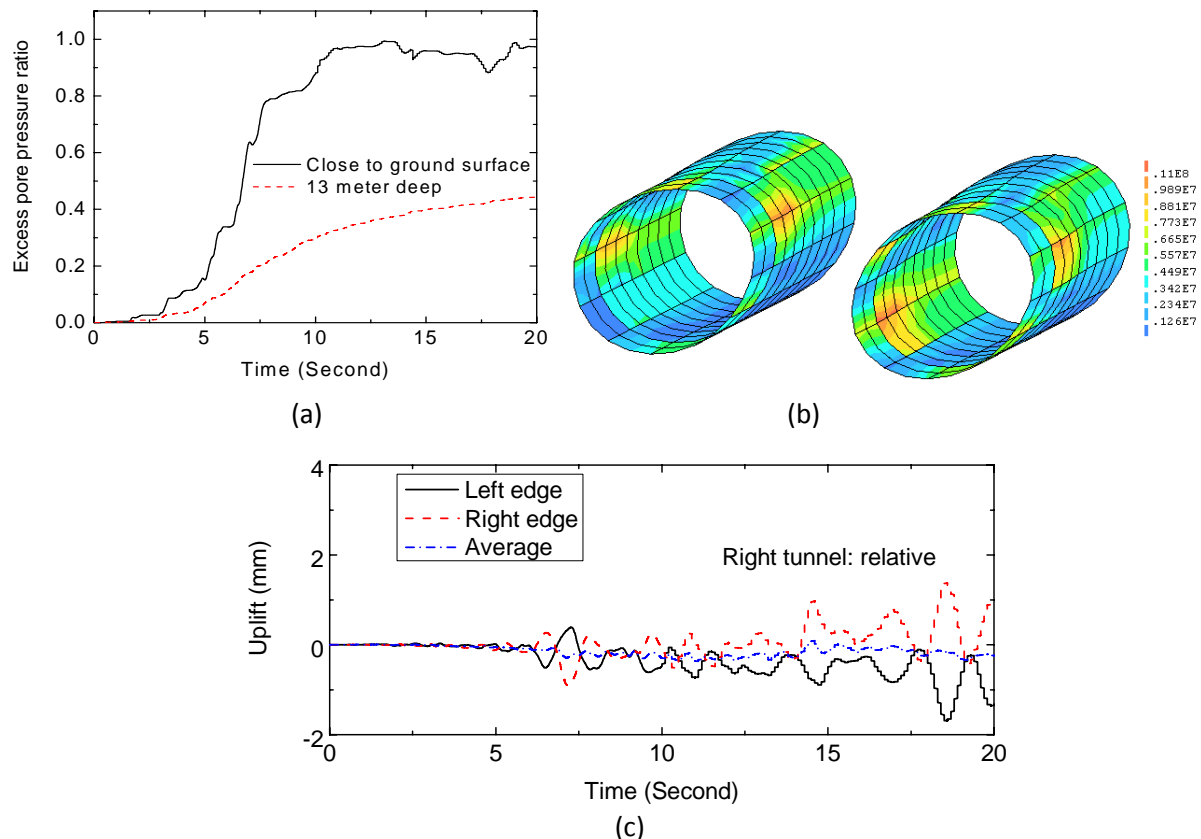


Fig. 11 Some responses of the tunnel-ground system under New York motion I: (a) Excess pore pressure ratio; (b) Maximum Mises stress in the tunnels; (c) Vertical displacement of the left tunnel

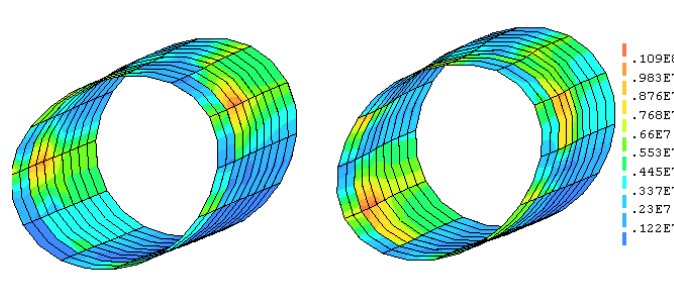
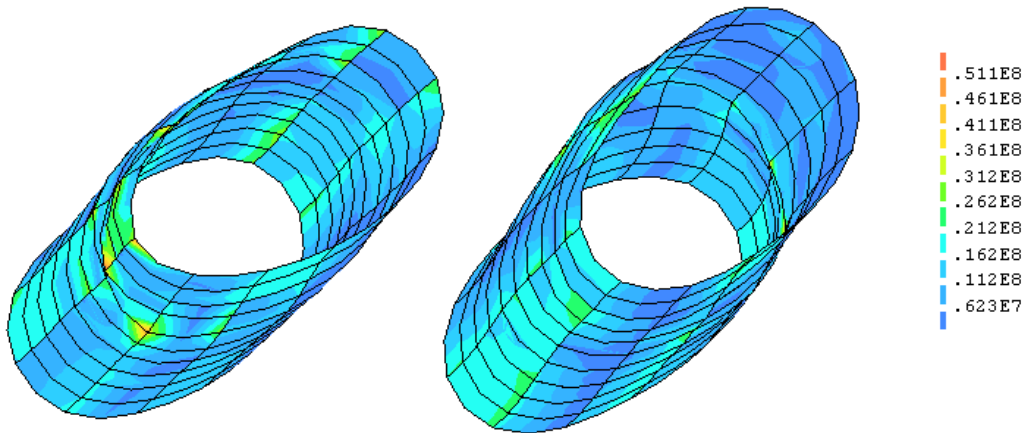


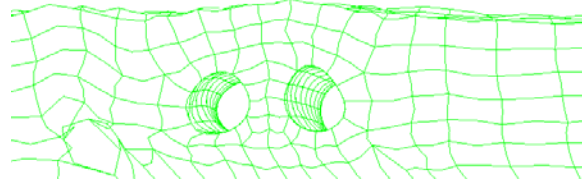
Fig. 12 Maximum von Mises stress in the tunnels under New York motion II

### 6 Effects of Soil Thickness

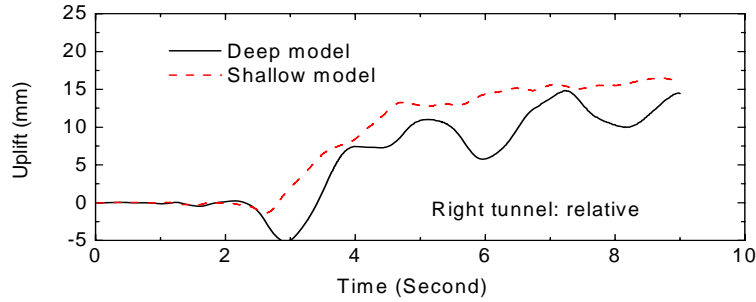
Under the Northridge motion, the deep model resulted in larger stress in the tunnels compared to the shallow model, as shown in Fig. 13a. The maximum von Mises stress occurred at around 5.6 second and was about 56 MPa. The larger stress is mainly due to the larger lateral deformation of the liquefied soil layer, as shown in Fig. 13b (comparing to Fig. 8b). The relative vertical deformation in the tunnels was actually smaller for the deep model, as can be seen in Fig. 13c.



(a)



(b)



(c)

Fig. 13 Seismic response of the deep model under the Northridge motion: (a) Maximum von Mises stress; (b) Front deformed mesh at 9 second (enlarged 35 times); (c) Comparison of uplift

Under New York motion II, the maximum von Mises stress in the tunnels was also larger with the deep model, as shown in Fig. 14. The maximum von Mises stress was around 18 MPa, compared to 12 MPa using the shallow model under the same excitation. This increase was also due to the increase in the horizontal deformation of soils.

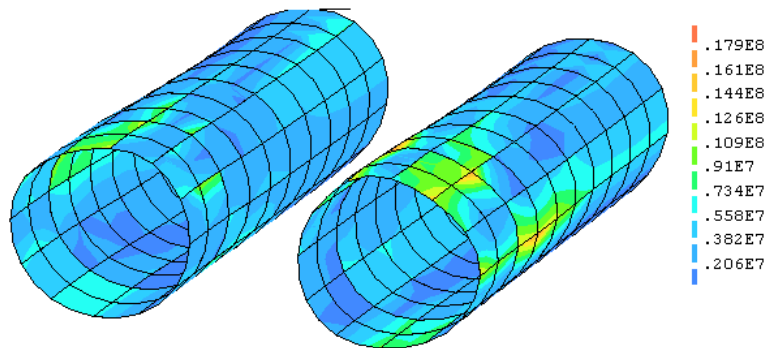


Fig.14 Maximum von Mises stress in the tunnels due to New York motion II with the deep model

## 7 Conclusions

Three dimensional (3D) Finite Element analysis was carried out to investigate the seismic response of underground tunnels subject to earthquake loading considering the effects of excess pore pressure and soil liquefaction. Twin subway tunnels at a diameter of 5 meter, the lining of which was made of grey cast-iron at a thickness of 6.5 cm, were considered in this study. The soils were simulated using Nishi soil liquefaction model and interface elements were utilized to model soil-tunnel interaction. The present study focused on the 3D response of underground tunnels passing through both dense and loose grounds. Two sets of ground motions, a record from the 1994 Northridge earthquake and the synthesized New York City ground motions for bridges, both scaled to an  $a_{max}$  of 0.35 g, were used as inputs in the analysis. The effect of soil thickness over bedrock was also investigated.

It was found from the analysis that underground tunnels passing through both dense and loose saturated ground exhibited two distinctive deformation modes: the uplift and the lateral deformation

due to the difference in the soil liquefaction susceptibility. The tunnels were twisted due to these distinctive deformation modes and the maximum stress in the tunnels occurred in a region close to the boundary between dense and loose grounds. Comparatively, the analysis results indicated that lateral soil deformation contributed more to the stress in the tunnels than the uplift. It was also found that when soil liquefaction was not extensive in the ground, the tunnels settled instead of uplifted.

Although scaled to the same maximum acceleration, the Northridge motion induced much larger responses in the ground-tunnel system than the New York motions. It is believed that the difference was attributed to the very different frequency characteristics of the two sets of motions. For soil liquefaction problems, motion with larger dominant frequency would lead to much more extensive soil liquefaction and much larger stress in the tunnels. It was also found that the synthesized motions from the same design response spectrum might still result in different stresses in the tunnels, indicating that in the design of underground tunnels sufficient number of synthesized motions that are compatible with the design spectrum in the area should be analyzed in order to take into account the ground motion uncertainty.

Preliminary analysis also showed that deep soil, at least in the range investigated, led to larger response in the tunnels. It is postulated that this effect is also related to the frequency characteristics of input motions and should be further investigated.

### **Acknowledgement**

The present study was supported by the United States Department of Transportation (USDOT) through a mini-grant awarded to the author by University Transportation Research Center – Region II. The support is gratefully acknowledged.

## References

- [1] Hall WJ and O'Rourke TD. Seismic behaviour and vulnerability of pipelines. Lifeline earthquake engineering, ASCE, New York; 1991. pp. 761–73.
- [2] O'Rourke TD, Gowdy TE, Stewart HE and Pease JW. Lifeline and geotechnical aspects of the 1989 Loma Prieta Earthquake. Proceedings of the 2nd international conference on recent advances in geotechnical earthquake engineering and soil dynamics, University of Missouri-Rolla, Rolla (MO); 1991. pp. 1601–1612.
- [3] Mohri Y, Yasunaka M and Shigeru T. Damage to buried pipeline due to liquefaction induced performance at the ground by the Hokkaido–Nansei–Oki earthquake in 1993. Proceedings of the 1st international conference on earthquake geotechnical engineering, Balkema, Rotterdam, The Netherlands; 1995. pp. 31–36.
- [4] Sasaki T, Koseki J, Matsuo O, Saito K, Yamashita M. Analyses of damage to sewer pipes in Shibetsu Town during the 1994 Hokkaido–Toho–Oki earthquake. In: Proceedings of the 1999 5th US conference on lifeline earthquake engineering: optimizing post-earthquake lifeline system reliability, Seattle (WA), USA; 1991. pp 247–56.
- [5] Shinozuka M, Ballantyne D, Borchardt R, Buckle I, O'Rourke TD, Schiff A. The Hanshin–Awaji earthquake of January 17, 1995 Performance of lifelines. Technical Report Prepared for NCEER, Buffalo (NY); 1995.
- [6] Tsai J, Jou L and Lin SH. Damage to buried water supply pipelines in the Chi–Chi (Taiwan) earthquake and a preliminary evaluation of seismic resistance of pipe joints. J Chin Inst Eng, Trans Chin Inst Eng 2000; 23(4): 395–408.
- [7] Schmidt B and Hashash YST. US immersed tube retrofit. Tunnels Tunneling Int 1998; 30(11): 22–24.
- [8] Wang LRL, Shim JS, Ishibashi I and Wang Y. Dynamic responses of buried pipelines during a liquefaction process. Soil Dyn Earthquake Eng 1990; 9(1): 44–50.
- [9] Koseki J, Matsuo O and Koga Y. Uplift behavior of underground structures caused by liquefaction of surrounding soil during earthquake. Soils Foundations 1997; 37: 97–108.
- [10] Orense RP, Morimoto I, Yamamoto Y, Yumiyama T, Yamamoto H and Sugawara K. Study on wall-type gravel drains as liquefaction countermeasure for underground structures. Soil Dyn Earthquake Eng 2003; 23(1): 19–39.

- [11] Ling HI, Mohri Y, Kawabata T, Liu L, Burke C and Sun L. Centrifugal modeling of seismic behavior of large-diameter pipe in liquefiable soil. *J Geotech Geoenviron Eng, ASCE* 2003; 129 (12): 1092–1101.
- [12] Khoshnoudian F and Shahrour L. Numerical analysis of the seismic behaviour of tunnels constructed in liquefiable soils. *Soils Foundations* 2002; 42 (6): 1–8.
- [13] Yang D, Naesgaard E, Byrne PM, Adalier K and Abdoun T. Numerical model verification and calibration of George Massey Tunnel using centrifuge models, *Can Geotech J* 2004; 41: 921–942.
- [14] Taylor PR, Ibrahim HH and Yang D. Seismic retrofit of George Massey Tunnel. *Earthquake Eng Struct Dyn* 2005; 34: 519–542.
- [15] Liu H and Song E. Seismic response of large underground structures in liquefiable soils subjected to horizontal and vertical earthquake excitations. *Comput Geotech* 2005; 32(4): 223–244.
- [16] Liu H and Song E. Working mechanism of cutoff walls in reducing uplift of large underground structures induced by soil liquefaction. *Comput Geotech* 2006; 33(4-5): 209–221.
- [17] Azadi M and Mir Mohammad Hosseini SM. Analyses of the effect of seismic behavior of shallow tunnels in liquefiable grounds. *Tunnelling and Underground Space Technology* 2010; 25(5): 543–552.
- [18] Azadi M and Mir Mohammad Hosseini SM. The uplifting behavior of shallow tunnels within the liquefiable soils under cyclic loadings. *Tunnelling Underground Space Technol* 2010; 25(2): 158-167.
- [19] Chou JC, Kutter BL, Travasarou T and Chacko JM. Centrifuge modeling of liquefaction-induced uplift for the BART transbay tube. *J Geotech Geoenviron Eng, ASCE* 2011; in press.
- [20] Chou HS, Yang CY, Hsieh BJ and Chang SS. A study of liquefaction related damages on shield tunnels. *Tunnelling Underground Space Technol* 2001; 16(3): 185–193.
- [21] Tanaka H, Kita H, Iida T, Saimura Y. Countermeasure against liquefaction for buried structures using sheet pile with drain capacity. *Earthquake geotechnical engineering*. Rotterdam, The Netherlands: Balkema; 1995. p. 999–1004.
- [22] Hashash YMA, Hook JJ, Schmidt B, Yao J. Seismic design and analysis of underground structures. *Tunnelling Underground Space Technol* 2001;16(4):247–93.
- [23] Ninomiya Y, Hagiwara R, Azuma T. Rise of excess pore water pressure and uplift of underground structures due to liquefaction. *Earthquake geotechnical engineering*. Rotterdam, The Netherlands: Balkema; 1995. p. 1023–28.
- [24] St John CM, Zahrah TF. Aseismic design of underground structures. *Tunnelling Underground Space Technol* 1987; 2(2): 165–97.

- [25] Ohshima Y, Watanabe H. Elasto-plastic dynamic response analysis of underground structure-soil composite based upon the 3-D finite element method. *Struct Eng/Earthquake Eng* 1994;11(2):1035–145.
- [26] Stamos AA, Beskos DE. Dynamic analysis of large 3-D underground structures by the BEM. *Earthquake Eng Struct Dyn* 1995;24(6):917–34.
- [27] Hashash YMA, Hook JJ, Schmidt B, Yao J. Seismic design and analysis of underground structures. *Tunnelling Underground Space Technol* 2001;16(4):247–93.
- [28] Amorosia A and Boldinib D. Numerical modelling of the transverse dynamic behaviour of circular tunnels in clayey soils. *Soil Dyn Earthquake Eng* 2009; 29(6): 1059–1072.
- [29] Tajimi M. Damage done by the great earthquake disaster of the Hanshin-Awaji district to the Kobe Municipal Subway System and restoration works of the damage. *Jpn Railway Eng* 1996;137:19–23.
- [30] Rossum L. New York City transportation tunnels—case histories and designer’s approach. *Munic Eng J* 1985; 71:1–24.
- [31] TNO DIANA BV. DIANA Finite Element Analysis User’s Manual, version 9.4.2, 2010.
- [32] Nishi K and Kanatani M. Constitutive relations for sand under cyclic loading based on elasto-plasticity theory. *Soils Foundations* 1990; 30(2): 43-59.
- [33] Cazemier W, Feenstra P H, Snijders JMA, Visschedijk MAT, Bezuijen A, Teunissen JMA, van Kesteren WGM and Meijer K. TNO Liquefaction Project Definition Study. Tech. Rep. 97-NM-R1449, TNO Building and Construction Research, 1998.
- [34] Ghaboussi J, Hansmire WH, Parker HW and Kim KJ. Finite element simulation of tunneling over subways. *J Geotech Eng ASCE* 1983; 109:318–334.
- [35] Risk Engineering Inc. Seismic Hazard for New York City. Final Report To Weidlinger Associates, 2002.
- [36] 2010 Edition NEHRP Recommended Provisions for Seismic Regulations for New Buildings and Other Structures, prepared by the New Building Seismic Safety Council for the Federal Emergency Management Agency, Washington D.C.
- [37] AASHTO. Guide Specifications for LRFD Seismic Bridge Design, 2009, 1st Edition.

## **Appendix I Nishi liquefaction model**

The Nishi model uses the relative shear stress level:

$$\eta_{ij} = \frac{\sigma_{ij} - \frac{1}{3}\sigma_{kk}\delta_{ij}}{\frac{1}{3}\sigma_{kk}} \quad (\text{AI.1})$$

Based on this definition, two quantities related to the stress history are defined:

$\eta_{ij}^0$  : the initial relative stress level,

$\eta_{ij}^r$  : the relative stress ratio at the last reversal point under cyclic loading.

Related to these two stress levels are two stress invariants:

$$\eta^* = \sqrt{(\eta_{ij} - \eta_{ij}^0)(\eta_{ij} - \eta_{ij}^0)} \quad (\text{AI.2})$$

$$\eta^{r*} = \sqrt{(\eta_{ij} - \eta_{ij}^r)(\eta_{ij} - \eta_{ij}^r)} \quad (\text{AI.3})$$

The strain is split up into the elastic and plastic components:

$$\varepsilon_{ij} = \varepsilon_{ij}^e + \varepsilon_{ij}^p \quad (\text{AI.4})$$

And the plastic deviatoric strain is defined as:

$$e_{ij}^p = \varepsilon_{ij}^p - \frac{1}{3}\varepsilon_{kk}\delta_{ij} \quad (\text{AI.5})$$

The elastic behavior of the model is defined by the Poisson's ratio  $\nu$  and the bulk modulus  $K$ , which is expressed as:

$$K = \frac{\sigma'_m}{k^*} \quad (\text{AI.6})$$

Here  $\sigma'_m = \frac{1}{3}\sigma'_{kk}$  is the mean effective stress of soil.

The plastic strain component through the following equation:

$$d\varepsilon_{ij}^p = B_{ijkl}d\sigma_{kl} \quad (\text{AI.7})$$

The plastic compliance tensor is written as:

$$B_{ijkl}^p = \frac{1}{\sigma'_m G^* \left(1 - \theta \frac{\eta^*}{M_f}\right)^2} \left( \xi_{ij} + \alpha(M_m - \eta^*) \frac{\delta_{ij}}{3} \right) \left( \xi_{kl} - \eta_{mn} \xi_{mn} \frac{\delta_{kl}}{3} \right) \quad (\text{AI.8})$$

In this equation,  $M_f$  is the relative stress ratio at failure determined by  $\phi$ , and  $M_m$  is the relative stress ratio under maximum volumetric compression determined by  $\phi_p$ .

$\xi_{ij}$ ,  $\alpha$  and  $\theta$  all depend on the stress state:

When the maximum relative stress ratio is increasing and the maximum stress ratio ever reached the present stress ratio,  $\alpha = 1$ ,  $\theta = 1$  and

$$\xi_{ij} = \frac{\eta_{ij} - \eta_{ij}^0}{\eta^*} \quad (\text{AI.9})$$

When reverse loading occurs the present relative stress ratio is smaller than the maximum one ever reached,  $\theta = 0.5$ ,

$$\xi_{ij} = \frac{\eta_{ij} - \eta_{ij}^r}{\eta^{r*}} \quad (\text{AI.10})$$

and

$$\alpha = 1 - \frac{\varepsilon_{kk}^p}{m^* \sigma_m^r (\eta^{r*})^n} \quad (\text{AI.11})$$

Here  $m^*$  and  $n$  are both material constants.

Finally the last variable in Eq. (AI.8)  $G^*$  is defined as:

$$G^* = G_0^* \exp(-\beta_1 d_m^r) \quad (\text{AI.12})$$

$$d_m^r = \max\left(\left|\sum_{i=1}^m -1^{i+1} (d_i^r - d_{i-1}^r)\right|, d_m^r\right) \quad (\text{AI.13})$$

Here  $m$  is the number of stress reversals.  $d = \int de_{ij} de_{ij}$  and is the equivalent plastic strain, and  $d_m^r$  the maximum one at the last stress reversal, measured from the initial state.  $G_0^*$  is a material constant.

## Appendix II Interface Elements

The interface between soil and structures in this study was described by two components: the elastic component and the slippage component. The elastic behavior is expressed as:

$$\begin{Bmatrix} t_n \\ t_t \\ t_s \end{Bmatrix} = \begin{bmatrix} D_{nn} & & \\ & D_{tt} & \\ & & D_{ss} \end{bmatrix} \begin{Bmatrix} \Delta u_n \\ \Delta u_t \\ \Delta u_s \end{Bmatrix} \quad (\text{AII.1})$$

Here the tractions  $t$  on the interface is related to the gap displacement  $\Delta u$  through three stiffness parameters. In the TNO-DIANA program, the two tangential stiffness parameters  $D_{tt}$  is assumed to be the same as  $D_{ss}$ . When the slippage of interface occurs when

$$\sqrt{t_n^2 + t_t^2} = c + t_n \tan \delta \quad (\text{AII.2})$$

Here  $c$  is the interface cohesion and  $\delta$  is the interface friction angle.